Image Reconstruction of Moderate Contrast Targets Using the Distorted Born Iterative Method

Roberto Lavarello and Michael Oelze
Bioacoustics Research Laboratory
Department of Electrical and Computer Engineering
University of Illinois at Urbana-Champaign
Urbana, IL 61801
Email: lavarell@uiuc.edu

***Abstract*— Ultrasonic tomography using inverse scattering, i.e., the distorted Born iterative method (DBIM), allows for the quantitative image reconstruction of mechanical properties of materials. The use of multi-frequency information has been proposed to avoid convergence issues for targets with moderate speed of sound contrasts Δc (i.e., targets for which the excess phase $\Delta\phi$ when propagating through the object is larger than π) but not validated experimentally. Furthermore, DBIM has to be regularized due to its ill-conditioning. To experimentally validate DBIM for use in ultrasonic tomography, a systematic procedure to choose the regularization parameter based on the Rayleigh quotient iteration was developed and images of objects with moderate Δc were reconstructed. The performance of DBIM using the developed regularization scheme was studied through: 1) Simulations of a two dimensional (2D) phantom ($\Delta\phi = 2.14\pi$) with inclusions smaller than a wavelength, 2) Experiments with a balloon phantom with high Δc with scattered data collected at 0.64 MHz ($\Delta\phi$ = 0.84π) and 1.2 MHz ($\Delta\phi$ = 1.6π), and 3) Three dimensional (3D) reconstruction of a moderate contrast sphere ($\Delta\phi = 1.32\pi$). The 2D and 3D multi-frequency DBIM simulations were successfully stabilized by the proposed regularization scheme as evidenced by the low reconstruction mean square errors (MSEs) (Δc MSE = 9% for 2D and 15% for 3D) and the detection of the sub-wavelength inclusions in the 2D reconstruction. In experiments, the measured scattered fields agreed well with the predicted scattered fields from the phantom model (MSE = 4% for 0.64 MHz and MSE = 7.8% for 1.2 MHz). The MSE of the reconstructed image using only the experimental data at 0.64 MHz was 19%. Using the experimental data at 1.2 MHz to refine the 0.64 MHz reconstruction allowed the MSE to be reduced to 12%, and improved the spatial resolution as evidenced by the reduced edge blurring.**

I. Motivation

Ultrasonic tomography using inverse scattering methods, i.e., the distorted Born iterative method (DBIM), allows for quantitative image reconstruction of mechanical properties of materials. The use of multi-frequency information has been proposed to avoid convergence issues for targets with moderate speed of sound contrasts Δc (i.e., targets for which the excess phase $\Delta\phi$ when propagating through the object is larger than π) but not validated experimentally. Furthermore, DBIM has to be regularized due to its ill-conditioning. The present work introduces a robust, computationally efficient regularization scheme to be used with DBIM and both simulations and experimental validation to assess its performance.

II. Inverse Scattering and the DBIM

The details of DBIM [1] are presented here for completeness. For the special case of constant density, the integral wave equation can be written as

$$p(\vec{r}) = e_s(\vec{r}) + \int_\Omega d\vec{r}\,'\mathcal{O}(\vec{r}\,')p(\vec{r}\,')G_0(\vec{r},\vec{r}\,') \qquad (1)$$

where Ω is the computational domain, $p(\vec{r})$ is the acoustical pressure, $e_s(\vec{r})$ is the incident field caused by a source located at $\vec{r}_s$, $s = 0, 1, ..., N_s$, $\mathcal{O}(\vec{r}) = \left[k^2(\vec{r}) - k_0^2\right]$ is known as the object function with $k(\vec{r})$ the wave number function, $G_0(\vec{r},\vec{r}\,')$ is the wave propagation Green's function, and $\vec{r}$ is the position vector.

The object is divided into N subscatterers centered at positions $\vec{r}_m$, $m = 0, 1, ..., N$. Using delta testing functions, (1) can be evaluated at all points $\vec{r}_m$ which results in the system of equations

$$\bar{p}_s = \left[\bar{I} - \bar{C}\cdot\mathcal{D}(\bar{\mathcal{O}})\right]^{-1}\cdot\bar{e}_s \qquad (2)$$

where $\mathcal{D}(\cdot)$ is an operator that transforms an Nx1 vector into an NxN diagonal matrix, $\bar{\mathcal{O}}$, $\bar{p}_s$, and $\bar{e}_s$ are Nx1 vectors containing the values of the object function and the total and incident acoustic pressure at points $\vec{r}_m$ when the source is placed at $\vec{r}_s$, respectively, and $\bar{C}$ is an NxN matrix whose elements are given by $\left[\bar{C}\right]_{mn} = G_m(\vec{r}_n)$, with

$$G_m(\vec{r}) = \int d\vec{r}\;G_0(\vec{r},\vec{r})\;b_m(\vec{r}) \qquad (3)$$

Using delta testing functions to evaluate (1) at the receiver positions $\vec{r}_r$, $r = 1, 2, ..., N_r$, the scattered field can be calculated as

$$\bar{p}_s^{sc} = \bar{D}\cdot\mathcal{D}(\bar{\mathcal{O}})\cdot\bar{p}_s \qquad (4)$$

where $\bar{D}$ is an N_rxN matrix whose elements are equal to $\left[\bar{D}\right]_{rm} = G_m(\vec{r}_r)$. In contrast, if the object function is not known then (1) cannot be solved because the acoustic field inside the scatterer cannot be calculated. Therefore, the object function must be obtained using an iterative method. First, a trial object function $\mathcal{O}_{(n)}$ is chosen for which the corresponding vectors $\bar{p}_s^{sc}$ and $\bar{p}_s$ are calculated. Next, the object function is updated as $\bar{\mathcal{O}}_{(n+1)} = \bar{\mathcal{O}}_{(n)} + \Delta\bar{\mathcal{O}}_{(n)}$, where $\Delta\bar{\mathcal{O}}_{(n)}$ is given by the regularized optimization problem

$$\Delta\mathcal{O}_{(n)} = \arg\min_{\Delta\mathcal{O}} ||\Delta\bar{p}^{sc} - \bar{F}_{(n)} \cdot \Delta\mathcal{O}||_2^2 + \alpha||\Delta\mathcal{O}||_2^2, \quad (5)$$

where $\Delta\bar{p}^{sc}$ is the difference between the predicted $\bar{p}^{sc}$ and measured $\bar{p}_m^{sc}$ scattered fields, α is the regularization parameter, and $\bar{F}_{(n)}$ is the Frechet derivative matrix, which is composed of N_s stacked matrices $\bar{F}_s$ of the form [2]

$$\bar{F}_s = \bar{D} \cdot \left\{\bar{I} - \mathcal{D}(\bar{\mathcal{O}}) \cdot \bar{C}\right\}^{-1} \cdot \mathcal{D}(\bar{p}_s). \quad (6)$$

III. Proposed Regularization Method

Several methods to determine the optimum α for matrix equations are available in the literature, such as the L-curve [3] or the generalized cross validation (GCV) [4]. However, this methods have a large computational cost and potential detrimental effects on the convergence of DBIM. Some other approaches to find α for inverse scattering can be found in the literature [5]–[8], but they depend on heuristic choices of independent parameters and therefore it is not clear how to use them in general scenarios. Therefore, a systematic and yet efficient approach to select the regularization parameter needs to be developed. The initial regularization parameter α is chosen to be comparable to the square of the first singular value σ_0 of the Frechet derivative matrix. This choice is sufficient to avoid rapid variations in the initial reconstructed profiles, which have been found to be critical to the convergence of inverse scattering algorithms. As the relative residual error (RRE) decreases, the value of the regularization parameter can be relaxed to allow for contributions from higher frequencies. Because of simplicity, the relaxation process used in this work is based on RRE thresholding. The proposed scheme [9] is shown in Table I.

TABLE I
REGULARIZATION PARAMETER SELECTION SCHEME AS A FUNCTION OF THE FORWARD ERROR.

RRE	Regularization parameter α
0.5<RRE	$\sigma_0^2/2$
0.25<RRE≤0.5	$\sigma_0^2/20$
RRE≤0.25	$\sigma_0^2/200$

IV. Simulations and Experimental Results

Simulations were performed using the synthetic phantom shown in Fig. 1(a) with $\Delta\phi = 2.14\pi$ at the maximum frequency used. The reconstructed image shown in Fig. 1(b) was obtained using two frequencies to avoid divergence. The synthetic measurements were contaminated with 5% zero-mean Gaussian noise. The multi-frequency DBIM simulations were successfully stabilized by the proposed regularization scheme as evidenced by the low reconstruction mean square error (MSE) (Δc MSE = 9%) and the detection of the sub-wavelength inclusions.

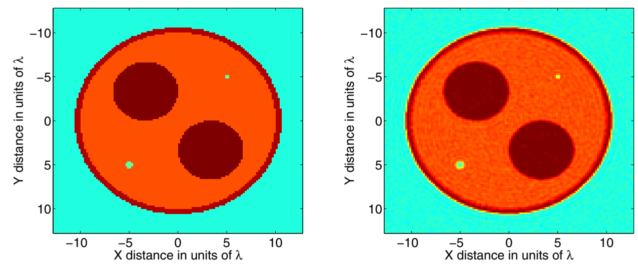

Fig. 1. Ideal (left) and reconstructed (right) profiles for the 2D multi-frequency DBIM simulation using the proposed regularization scheme.

Experiments were conducted to validate the ability to perform DBIM inversions when dealing with real data collected using two circular, unfocused transducers. The first transducer was used as source and had a fixed position relative to the imaging target. The second transducer was used as receiver and rotated in a circular arc around the sample. Both transducers had a nominal center frequency of 1 MHz and reported radius of 0.0625 inches.

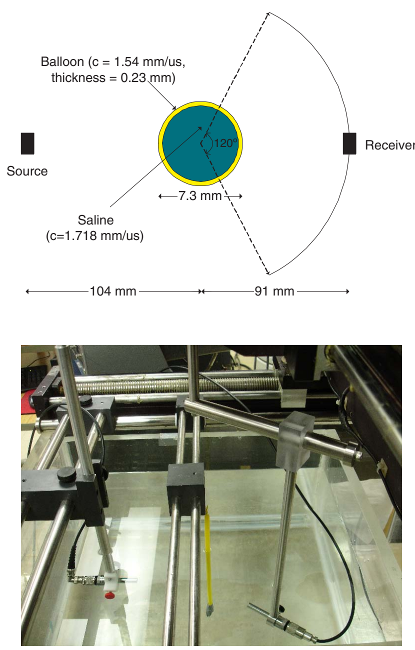

Fig. 2. Experimental configuration. Top: Schematic of the configuration setup. Bottom: Photograph of the experimental setup showing the source transducer (left), balloon phantom (middle), and receiver transducer attached to the rotating arm (right).

The imaging targets were phantoms built using soft rubber balloons filled with a saline solution.The saline solution was obtained by diluting 25 grams of salt in 100 milliliters of water. The speed of sound and thickness of the balloons and the speed of sound of the saline were estimated to be 1.54 mm/μs, 0.23 mm, and 1.718 mm/μs using time of flight measurements. The diameter of the inflated balloon was measured to be 7.3 mm.

The actual scanning configuration is shown in Fig. 2. The distances between the phantom and the source and receiver transducers were 104 mm and 91 mm, respectively. The

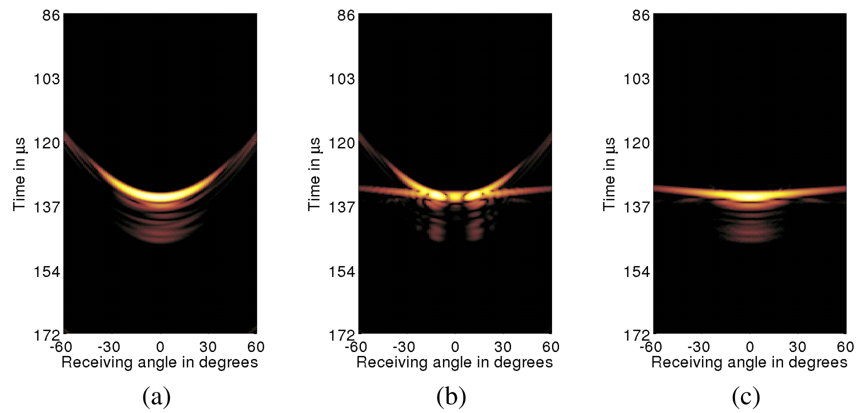

Fig. 3. Envelope of the measured pressure signals in decibel scale with a dynamic range of 40 dB as a function of the receiving angle. a) Incident field. b) Total field. c) Scattered field, calculated as the difference of (b) and (a).

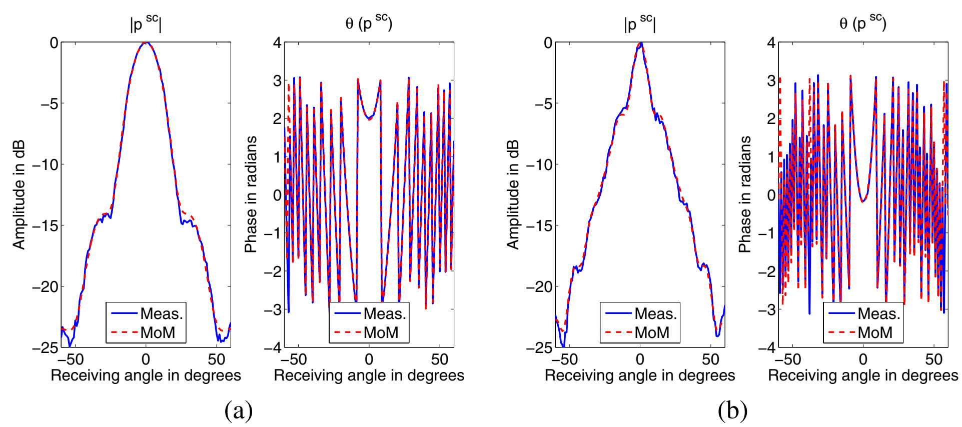

Fig. 4. Magnitude in dB (left column) and phase in radians (right column) of the scattered pressure at (a) 0.64 MHz and (b) 1.2 MHz. Both the measured (solid line) and MoM (dashed line) data are shown.

receiver transducer was mounted on a vertical rod, which was attached to an L-shaped mechanical element with adjustable horizontal length. With this arrangement, rotating the vertical segment of the L-shaped element resulted in the transducer describing a circular arc around the balloon phantom with radius given by the length of the horizontal segment. The receiving angle was changed between -60 and 60 degrees.

Two sets of measurements were collected: one without the sample in the water tank to measure the incident field, and one with the sample in the tank to measure the total acoustic field in the presence of the scatterer. The scattered field is obtained by subtracting the incident field from the total field. The three fields are shown in Fig. 3 as a function of the receiving angle.

The scattered fields at frequencies of interest were obtained by taking the Fourier transform of the measured waveforms for all receiver positions. A frequency of 1.2 MHz was chosen for the DBIM reconstructions. At this frequency, $\Delta\phi \approx 1.6\pi$ according to the phantom model, and therefore frequency hopping was required. A lower frequency of 0.64 MHz, for which $\Delta\phi \approx 0.85\pi$, was used for the coarse reconstruction. Figure 4 shows the measured scattered fields as a function of the receiver angle. For comparison, the ideal scattered field was also generated using a method of moments (MoM) solver. The MSEs between the measured and expected scattered fields were 4.1% and 7.8% for 0.64 MHz and 1.2 MHz, respectively.

The phantom reconstructions are shown in Fig. 5. For comparison, the DBIM reconstruction using the scattered data generated using the MoM solver was also calculated. Both reconstructions are in very good agreement. The MSE of the reconstructed image using only the experimental data at 0.64 MHz was 19%. Using the experimental data at 1.2 MHz to refine the 0.64 MHz reconstruction allowed the MSE to be reduced to 12%, and improved the spatial resolution as evidenced by the reduced edge blurring. The mean speed of sound and radius of the phantom were accurately reconstructed.

Three dimensional reconstructions of a sphere of radius 4λ and speed of sound contrast of 9% ($\Delta\phi = 1.32\pi$) were also obtained using two methods regularized with the scheme presented in this work. The reconstructions are shown in Fig. 6. In the first approach, simulated rectangular transducers focused on elevation with focal number of 4 were used to produce a series of 2D image slices of the object using 2D DBIM. The resulting 3D image reconstruction was rendered by stacking the serial 2D slices. The reconstruction MSE

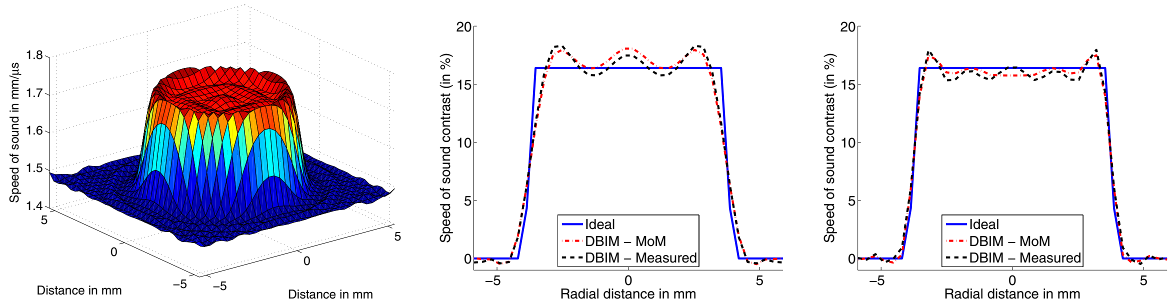

(a) (b) (c)

Fig. 5. DBIM reconstructions of the balloon phantom. a) The reconstructed speed of sound profile using DBIM and measured data. b) Profile of the reconstruction at 0.64 MHz. c) Profile of the reconstruction using 0.64 MHz and 1.2 MHz data. For (b) and (c), the ideal profile according to the model (solid line) and the DBIM reconstructions using ideal (dot-dashed line) and measured (dashed line) data are shown.

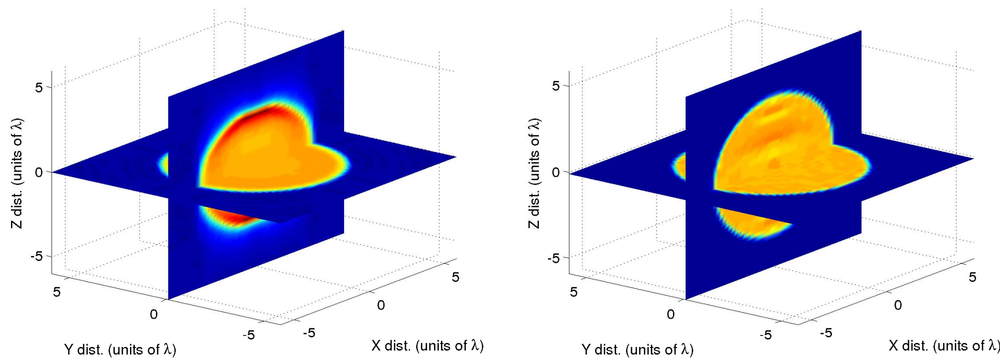

(a) (b)

Fig. 6. Three dimensional reconstructions of a sphere with radius 4λ and $\Delta c = 9\%$ using a) 2D stacking, b) 3D DBIM with frequency hopping.

was 31.6% and significant diffraction effects occured when the imaging plane did not pass through the center of the sphere. In the second approach, point-like transducers were simulated to produce a fully 3D DBIM image reconstruction using frequency hopping. The final reconstruction MSE was 15% and no significant diffraction effects at the edges of the sphere were observed.

V. Conclusions

A novel regularization approach for use in DBIM studies was presented. The approach was successfully tested using two and three dimensional simulations, and experiments with limited angular coverage. All these results indicate that the proposed regularization scheme is capable of producing accurate solutions even with reduced k-space coverage, without causing an excessive blurring of the reconstruction. The experimental results presented here are the first experimental validation of convergence of DBIM reconstructions for large contrast ($\Delta\phi > \pi$) with acoustic data using non-ambiguous imaging targets for which the validity of the reconstructions can be assessed.

VI. Acknowledgements

The authors would like to thank W.C. Chew, A. Hesford, S. Bond, and W.D. O'Brien, Jr. This work was partially funded by a grant from the 3M corporation.

References

[1] W.C. Chew and Y.M. Wang, "Reconstruction of two-dimensional permittivity distribution using the distorted Born iterative method," *IEEE Transactions on Medical Imaging*, vol. 9, no. 2, pp. 218–225, 1990.

[2] D. Borup, S. Johnson, W. Kim, and M. Berggren, "Nonperturbative diffraction tomography via Gauss-Newton iteration applied to the scattering integral equation," *Ultrasonic Imaging*, vol. 14, no. 1, pp. 69–85, 1992.

[3] P. C. Hansen, "Analysis of discrete ill-posed problems by means of the L-curve," *SIAM Review*, vol. 34, no. 4, pp. 561–580, 1992.

[4] G. H. Golub, M. Heath, and G. Wahba, "Generalized cross-validation as a method for choosing a good ridge parameter," *Technometrics*, vol. 21, pp. 215–223, 1979.

[5] O.S. Haddadin and E.S. Ebbini, "Adaptive regularization of a distorted Born iterative algorithm for diffraction tomography," in *IEEE International Conference on Image Processing*, vol. 2, 1996, pp. 725–728.

[6] Q.H. Liu, "Reconstruction of two-dimensional axisymmetric inhomogeneous media," *IEEE Transactions on Geoscience and Remote Sensing*, vol. 31, no. 3, pp. 587 – 594, 1993.

[7] A. Franchois and C. Pichot, "Microwave imaging - Complex permittivity reconstruction with a Levenberg-Marquardt method," *IEEE Transactions on Antennas and Propagation*, vol. 45, no. 2, pp. 203–215, 1997.

[8] G.L. Wang, W.C. Chew, T.J. Cui, A.A. Aydiner, D.L. Wright, and D.V. Smith, "3D near-to-surface conductivity reconstruction by inversion of VETEM data using the distorted Born iterative method," *Inverse Problems*, vol. 20, no. 6, pp. 195–216, 2004.

[9] R.J. Lavarello and M.L. Oelze, "A study on the reconstruction of moderate contrast targets using the distorted Born iterative method," *IEEE Transactions on Ultrasonics, Ferroelectrics, and Frequency Control*, accepted for publication.